crystals

MDPI

Article

Time-Resolved and Temperature-Dependent Fractional Amplitude Contributions to the Broadband Emission of CdSe Quantum Dots

Quinton Rice [1,2], Sangram Raut [3,4], Kyle Burney [1], Zygmunt Gryczynski [4], Ignacy Gryczynski [3], William W. Yu [5], Bagher Tabibi [1] and Jaetae Seo [1,*]

1 Advanced Center for Laser Science and Spectroscopy, Department of Physics, Hampton University, Hampton, VA 23668, USA; quinton.rice@uncp.edu (Q.R.); KyleBurney2@gmail.com (K.B.); bagher.tabibi@gmail.com (B.T.)
2 Department of Chemistry and Physics, The University of North Carolina at Pembroke, Pembroke, NC 28372, USA
3 Center for Fluorescence Technologies and Nanomedicine, Department of Cell Biology and Immunology, University of North Texas Health Science Center, Fort Worth, TX 76107, USA; sangramraut@gmail.com (S.R.); Ignacy.Gryczynski@unthsc.edu (I.G.)
4 Department of Physics and Astronomy, Texas Christian University, Fort Worth, TX 76129, USA; z.gryczynski@tcu.edu
5 Department of Chemistry and Physics, Louisiana State University, Shreveport, LA 71115, USA; william.yu@lsus.edu
* Correspondence: jaetae.seo@hamptonu.edu

Citation: Rice, Q.; Raut, S.; Burney, K.; Gryczynski, Z.; Gryczynski, I.; Yu, W.W.; Tabibi, B.; Seo, J. Time-Resolved and Temperature-Dependent Fractional Amplitude Contributions to the Broadband Emission of CdSe Quantum Dots. *Crystals* **2021**, *11*, 1284. https://doi.org/10.3390/cryst11111284

Academic Editors: Julien Brault, Felix Jaetae Seo, William Yu and Sanju Gupta

Received: 27 August 2021
Accepted: 12 October 2021
Published: 22 October 2021

Abstract: The broadband spontaneous emission of excitons in CdSe quantum dots (QDs) is of great interest for the spectral imaging of living organisms or specific substances in the visible spectral region as well as in the biological optical window near the infrared spectral region. Semiconductor QDs that are near the bulk Bohr radius exhibit wide spectral tunability and high color purity due to quantum confinement of excitons within the dot boundary. However, with reducing dot size, the role of the surface-trapped state increases. The temperature-dependent photoluminescence (PL) confirms this with a ~3:1 emission intensity decrease from the surface-trapped state compared to the band edge. Large crystal irregularity, dangling ions, and foreign molecules can introduce new electronic transitions from surface-trapped states that provide broad spontaneous emission in the spectral region from visible to near IR in addition to the band edge emission. The time-resolved PL analyzed the fractional contributions of band edge, surface-trapped states, and possible intermediate trapped states to the broad spectral emission in order to characterize the CdSe QDs.

Keywords: quantum dots; time-resolved spectroscopy

1. Introduction

Cadmium chalcogenide (Te, Se, and S) semiconductor quantum dots (QDs) typically possess high color purity, wide optical tunability, and large quantum yield in the visible and near infrared spectral region, which allows for various applications in photonics, LED and solar cell development, as well as optical sensing and bio-imaging [1–12]. The large quantum yield of cadmium chalcogenide colloidal QDs has been reported in the past two decades [13]. Exciton recombination is the origin of emission in CdSe QDs while the bandgap is tunable based on quantum confinement of the charge carriers. Bulk CdSe exhibits a bulk bandgap of 1.74 eV, while CdSe QDs near the bulk Bohr radius (~5.8 nm) displays large blue shift from the bulk bandgap. It is widely known that the bandgap is the main emission site for CdSe QDs; however other radiative transition may occur on the surface of the nanocrystal due to atomic vacancies, local lattice mismatches, adsorbates at the surface, dangling bonds, or imperfect crystallization during the time-sensitive synthesis process [14–16]. Incomplete crystalline structure can lead to defect sites which provide

more non-radiative channels during recombination. To enhance the quality and remove non-radiative decay in CdSe QDs, typically the surface defects are passivated with neutral ligands such as trioctylphosphine oxide (TOPO) or capped with high bandgap materials such as ZnS, which reduce non-radiative recombination and result in narrow spectral emission [17]. However, without such passivators or capping agents, the dangling bonds are free to exist and, consequently, surface defects are highly influential to the overall photoluminescence (PL) at longer wavelengths. Thus, tailoring to a specific spectral region is not only achieved by size control of the QDs during synthesis, but also by the defects present at the surface [18]. The PL of the QDs is strongly dependent on the surface-trapped state, which is itself largely affected by the chemical or physical interactions which take place on or near the surface of the QDs. Thus, the surface environment plays a crucial role in PL activation or quenching [14]. Interactions with the QD's surface-trapped state can be easily measured or observed through time-resolved and temperature-dependent PL studies. However, the surface-trapped state emission has a strong temperature dependence and gives broad emission due to the multiplicity of surface irregularities. While the temperature dependent bandgap is well known for bulk and QDs of CdSe, the dynamics of the surface-trapped state is less familiar.

In this article, temperature dependent PL measurements were performed to characterize the behavior of the bandgap and surface-trapped state of CdSe QDs. Time-resolved spectroscopy was also utilized to analyze the fractional contributions from the surface-trapped state to the overall PL.

2. Materials and Methods

The CdSe QDs were synthesized according to pre-established procedures [4]. The QDs in toluene were allowed to dry on a piece of cover glass and then placed on a thermally conducive arm and holder located within a vacuum chamber. A pressure gauge (Duniway Stockroom Corp., Model DTC-531-115-BX, Fremont, CA, USA) monitored the pressure drop to 20 mTorr via a mechanical vacuum pump. A closed helium refrigeration unit (Sumitomo CNA-11, Type SRDK-101 He, Tokyo, Japan) was then activated to bring the ambient temperature inside the chamber to 6 K, recorded with a temperature controller (Lakeshore 331, Westerville, OH, USA). Excitation source was supplemented with a HeCd laser (Melles Griot, Omnichrome Series 74, Carlsbad, CA, USA) operated at a wavelength of 442 nm with an average power reading of 31.7 mW. A beam chopper operated at 300 Hz was introduced before excitation. The optical spectra of the CdSe QDs were filtered using a 455 nm long wavelength pass filter and collected using an optical fiber (Ocean Optics P600-2-SR, Orlando, FL, USA) fed to a spectrometer (Ocean Optics, USB4E00675, Orlano, FL, USA) with a spectral range of 200–1100 nm and a resolution of 1 nm.

The time-resolved PL measurements of were performed utilizing a FluoTime 200 fluorometer (PicoQuant, Inc., Berlin, Germany) with a 470 nm diode laser excitation source with a pulse width of 120 ps and a 100 KHz repetition rate. The chosen PL measurement wavelengths were 575 nm, 675 nm, 750 nm, 815 nm, 815 nm, 855 nm, and 890 nm for the CdSe QD samples. The amplitude average lifetimes of CdSe QDs were determined using tail fitting of the multi-exponential equation and a nonlinear least square function to the decay measurements described in the literature [19–22], using the FluoFit4 program (PicoQuant, Inc., Berlin, Germany).

3. Results

In Figure 1, the absorption and PL spectra of CdSe QDs are displayed. The absorption features three prominent peaks at 551 nm, 515 nm, and 455 nm. According to Yu et al. [23,24], the calculated diameters of the nanocrystals in this study are ~3.1 nm. In Figure 1, the absorption spectrum shows the blue-shifted (QDs: 2.25 eV) bandgap of CdSe (Bulk: 1.74 eV) which is attributed to quantum confined carries near the bulk Bohr radius (5.8 nm for CdSe).

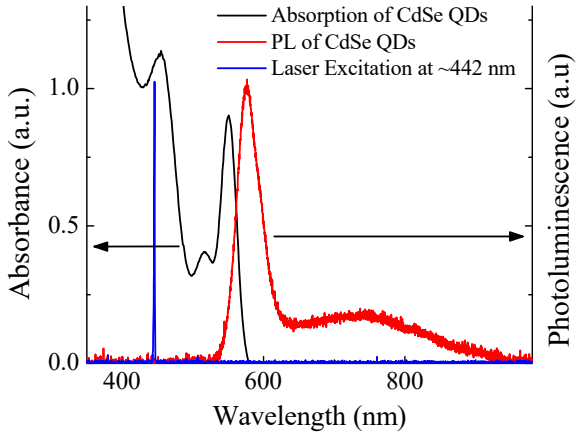

Figure 1. Absorption and photoluminescence spectra of CdSe QDs.

The PL peak observed at 576 nm originates from the band edge transition while the long tail spanning from 625 nm to 950 nm is due to the surface-trapped state transition. The surface-trapped state exists due to the surface irregularities formed during the crystal synthesis/growth processes. The PL from the surface-trapped state is attributed to carrier recombination at the defect sites, while the band edge transition is related to recombination closer to the bandgap. It is clear from the figure that the band edge transition dominates the PL spectra with 5-fold PL intensity compared to that of the surface-trapped state at room temperature. Figure 2 shows temperature dependent photoluminescence of CdSe QDs measured from 6 K to 300 K. The temperature dependent band edge transition at 568 nm at 6 K to 575 nm at 300 K was observed for increasing temperature in correspondence with the literature [25].

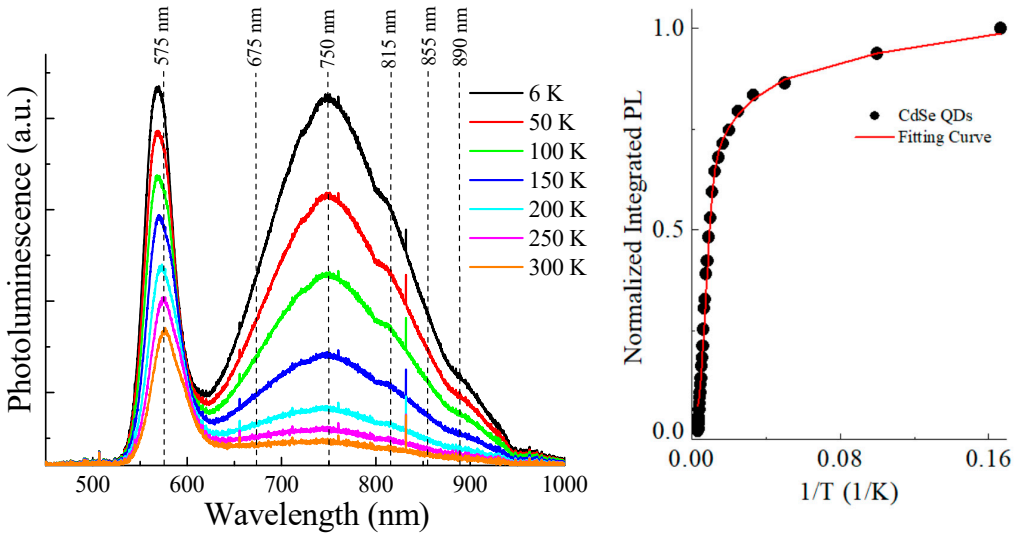

(**a**) (**b**)

Figure 2. (**a**) Temperature-dependent photoluminescence of CdSe QDs at select temperatures. (**b**) Integrated PL intensity as a function of the inverse temperature.

However, the band edge transition displayed a 2.6-fold decrease in emission intensity from 6 K to 300 K while the surface-trapped state displayed much more rapid thermal quenching with an 8.9-fold decrease in emission intensity from 6 K to 300 K. The surface-trapped state's emission intensity decreases 3.4 times faster with increasing temperature than the band edge transition. This may be due to the large number of non-radiative

recombination sites on the surface attributed to the numerous defects. While the bandgap is an intrinsic property of the semiconductor QDs, the surface-trapped state is heavily reliant upon the surface environment which, at room temperature, has higher non-radiative contributions compared with that of the band edge transition. The inset in Figure 2 displays the integrated PL intensity as a function of the inverse temperature for CdSe QDs. The fitting is based on the PL thermal quenching equation in the literature [11]. From the fitting, the fractional amplitudes (C_i) of activation ionization energy ($E_{act,i}$) are E_1~20.5 meV with C_1~0.7, E_2~26 meV with C_2~100, and E_3~50 meV with C_3~10 for CdSe QDs. The common phenomenon of PL thermal quenching is attributed to the increased non-radiative recombination probability of electrons and holes [26]. The radiative decay of CdSe QDs is further analyzed with time-resolved spectroscopy in order to specify the contributions from the surface-trapped state to the overall PL.

The temporal properties of CdSe QD emission which originate from the band edge and surface-trapped state transitions are investigated through time-resolved photoluminescence spectroscopy. In this study, the temporal decays were examined at six different observation wavelengths in order to account for the broad nature of the PL spectrum. Each observation wavelength exhibits a fast lifetime component (τ_1) related to the band edge to valence band transition, an intermediate lifetime component (τ_2) related to the surface-trapped state to valence band or band edge to valence trapped state transition and a slow lifetime component (τ_3) related to the surface-trapped state to valence trapped state transition. The fast component is heavily attributed to the band edge transition due to its relatively short lifetime and large fractional amplitude. As the band edge transition dominates the PL spectrum at room temperature, the largest fractional amplitude is accredited to the band edge. Time-resolved spectroscopy was performed at several observation wavelengths of 575 nm, 675 nm, 750 nm, 815 nm, 855 nm, and 890 nm shown in Figure 3a–f, respectively.

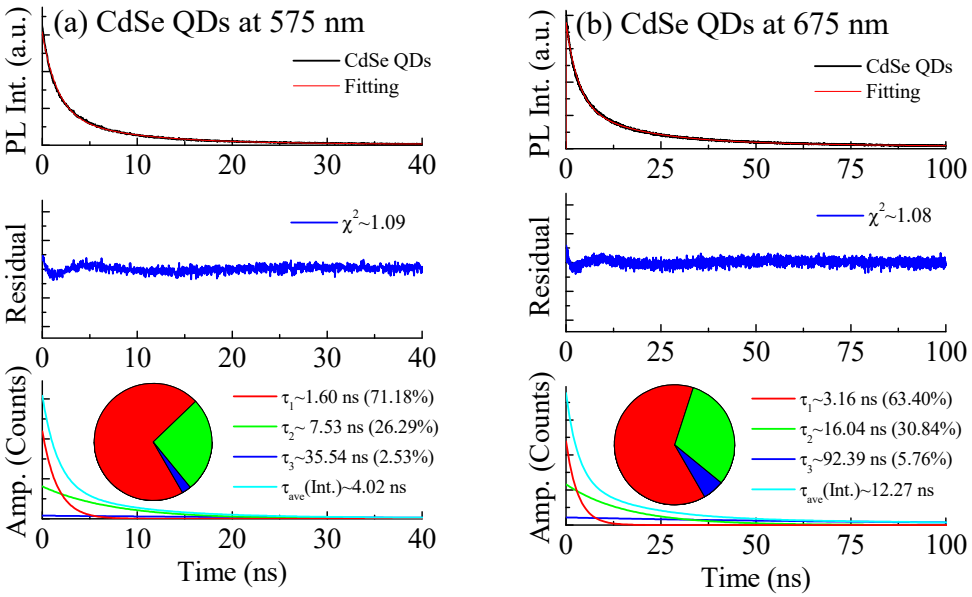

Figure 3. *Cont.*

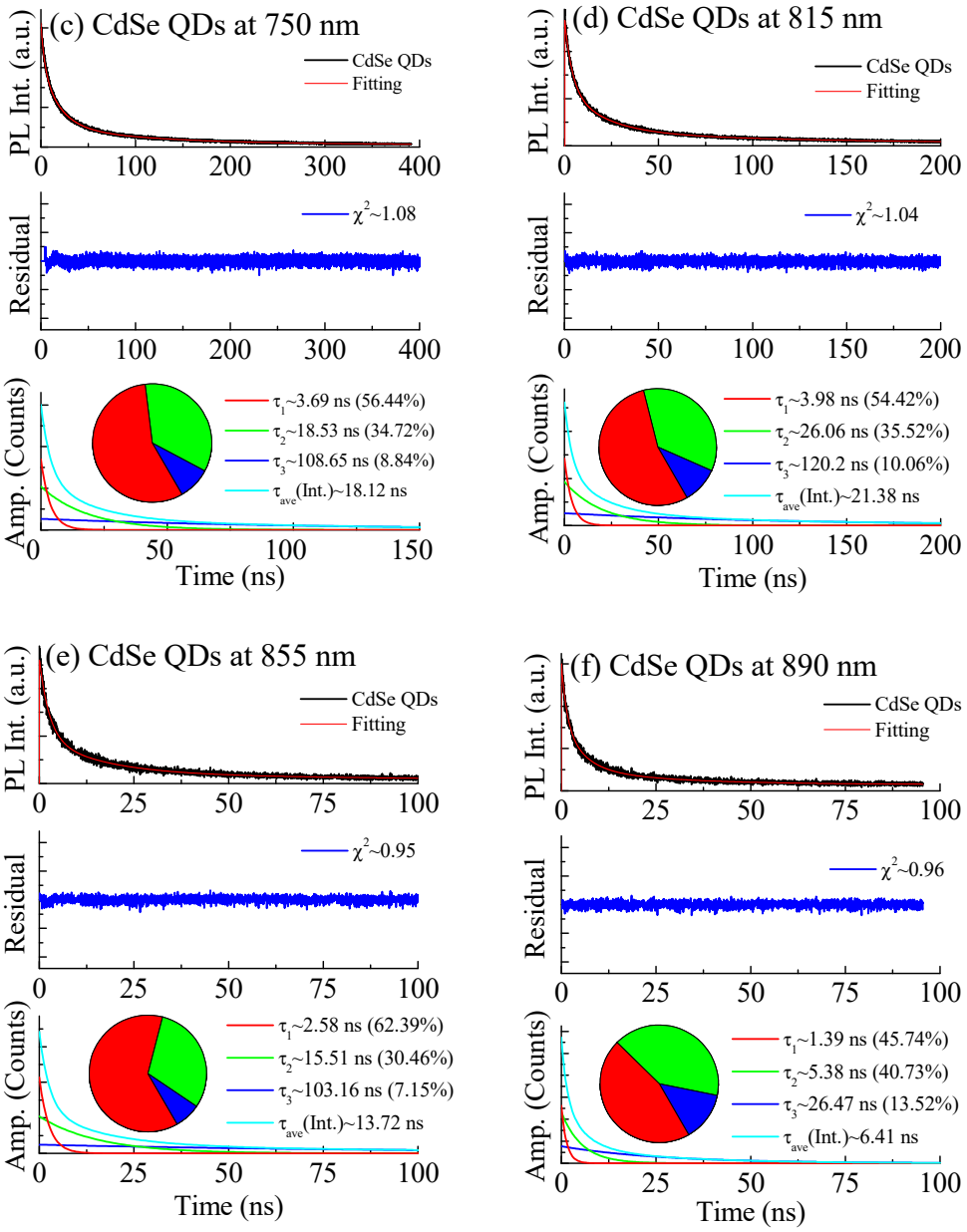

Figure 3. Time resolved PL of CdSe QDs at (**a**) 575 nm, (**b**) 675 nm, (**c**) 750 nm, (**d**) 815 nm, (**e**) 855 nm, and (**f**) 890 nm.

In Figure 3a, the lifetimes at 575 nm are τ_1~1.60 ns, τ_2~7.52 ns, and τ_3~35.54 ns with fractional amplitudes of 71.18%, 26.29%, and 2.53%, respectively. The large fractional amplitude of 71.18% indicates a strong influence from the band edge with noticeably less effect from the surface-trapped state which is reasonable considering the observation wavelength with respect to the PL spectrum in Figure 1. In Figure 3b, the lifetimes at 675 nm are τ_1~3.16 ns, τ_2~16.04 ns, and τ_3~92.39 ns with fractional amplitudes of 63.40%, 30.84%, and 5.76%, respectively. The observable drop in the fractional amplitude associated with the band edge transition from 71.18% at 575 nm to 63.40% at 675 nm is likely due to a higher contribution from the surface-trapped state at 675 nm. It is concluded that PL in this spectral region has obvious contributions from both band edge and surface-trapped state transitions however, the influence of the band edge to longer wavelengths is diminished. In Figure 3c, the lifetimes at 750 nm are τ_1~3.69 ns, τ_2~18.53 ns, and τ_3~108.65 ns with fractional amplitudes of 56.44%, 34.72%, and 8.84%, respectively. In this spectral region, the surface-trapped contribution is enhanced while the band edge

transition is further decreased as the observation wavelength is increased. In Figure 3d, the lifetimes at 815 nm are τ_1~3.98 ns, τ_2~26.06 ns, and τ_3~120.2 ns with fractional amplitudes of 54.42%, 35.52%, and 10.06%, respectively. While the trend of increased surface-trapped state contribution becomes more evident, Figure 3e displays an increased contribution from the band edge transition compared to Figure 3d. However, when compared to the overall surface-trapped state contribution of 36.6% (addition of fractional amplitudes from τ_1 and τ_2) from Figure 3b, the overall surface-trapped state contribution is 37.61% at 855 nm. While there may be some additional contribution from the band edge transition, the overall surface-trapped state contribution is increased in this spectral region. In Figure 3f, the lifetimes at 890 nm are τ_1~1.39 ns, τ_2~5.38 ns, and τ_3~26.47 ns with fractional amplitudes of 45.74%, 40.73%, and 13.52%, respectively. In this spectral region, the total trapped state (transitions not including band edge to valence band) contributions given by the total fractional amplitudes of τ_2 and τ_3 dominate the spectrum with combined fractional amplitude of 54.25%. This implies that, at 890 nm, the decay rate of the trapped state transitions is larger than that of the band edge transition; however, the band edge transition immensely influences the overall PL spectrum indicated by its high fractional contribution. The lifetimes of the band edge, surface-trapped state, and deeper trapped states have been explained by Jones et al. and Nirmal et al. through a dark exciton state or delayed exciton emission via thermalization of trapped states [27,28]. The average lifetime of the band edge transition is 30 times shorter than the average lifetime of the surface-trapped state transition. This suggests that the surface-trapped state has increased non-radiative contributions due to the defects on the surface of the nanocrystal, but the band edge transition is still the main contributor to the PL. This indicates that while the surface-trapped state provides the spectral coverage for broadband applications, the average lifetimes over the entire PL spectrum, remain fast due to the band edge dominance.

4. Conclusions

Temperature dependent PL spectra of CdSe QDs were studied for the purpose of developing efficient sensors and/or photonic devices. The wide PL spectrum qualifies them for various broadband applications resulting from the surface-trapped state contribution to the PL spectrum. The PL was observed to have a 3.5-fold contribution from the band edge transition compared to the surface-trapped state at room temperature. It was revealed through temperature dependent spectroscopy that the surface-trapped state exhibited strong thermal quenching with 8.9-fold decrease in emission intensity from 6 K to 300 K while the band edge transition displayed 2.6-fold decrease in emission intensity in the same temperature range. Time resolved spectroscopy further elucidated the dynamics of the surface-trapped state by exposing the large influence from the band edge transition to the entire PL spectrum while the surface-trapped state increasingly dominates in the longer wavelength spectral region. This indicates non-radiative decay at the surface-trapped state due to defects on the nanocrystal structure, which is also confirmed with an average lifetime 30 times longer than that of the band edge transition.

Author Contributions: Conceptualization, J.S.; Data curation, Q.R. and S.R.; Formal analysis, Q.R. and K.B.; Funding acquisition, B.T. and J.S.; Methodology, S.R., Z.G. and I.G.; Project administration, J.S.; Resources, W.W.Y. and J.S.; Supervision, B.T. and J.S.; Writing–original draft, Q.R. and K.B.; Writing–review & editing, Q.R., W.W.Y., B.T. and J.S. All authors have read and agreed to the published version of the manuscript.

Funding: The research at HU was funded by NSF HRD-1137747, ARO W911NF-11-1-0177, and NASA NNX15AQ03A. The work at UNT was supported by National Institutes of Health (NIH R01EB12003 and 5R21CA14897).

Data Availability Statement: Not applicable.

Acknowledgments: Not applicable.

Conflicts of Interest: The authors declare no conflict of interest.

References

1. Rice, Q.; Hayes, A.; Jung, S.; Wang, A.; Cho, H.; Kim, W.-J.; Abdel-Fattah, M.; Tabibi, B.; Seo, J. Plasmon-Coupled CdSe/ZnS and CdTe/CdS/ZnS Coreshells for Hybrid Light Emitting Devices. *J. Nanosci. Nanotechnol.* **2016**, *16*, 1942–1944. [CrossRef]
2. Khan, S.A.; Smith, G.T.; Seo, F.; Ellerbee, A.K. Label-Free and Non-Contact Optical Biosensing of Glucose with Quantum Dots. *Biosens. Bioelectron.* **2015**, *64*, 30–35. [CrossRef] [PubMed]
3. Kim, S.; Seo, J.; Ramdon, R.; Pyo, H.-B.; Song, K.; Kang, B.H. Solid-Phase Immunoassay of Polystyrene-Encapsulated Semiconductor Coreshells for Cardiac Marker Detection. *J. Nanomater.* **2012**, *2012*, 1–9. [CrossRef]
4. Seo, J.; Fudala, R.; Kim, W.-J.; Rich, R.; Tabibi, B.; Cho, H.; Gryczynski, Z.; Gryczynski, I.; Yu, W. Hybrid Optical Materials of Plasmon-Coupled CdSe/ZnS Coreshells for Photonic Applications. *Opt. Mater. Express* **2012**, *2*, 1026–1039. [CrossRef] [PubMed]
5. Mordant, D.J.; Al-Abboud, I.; Muyo, G.; Gorman, A.; Sallam, A.; Ritchie, P.; Harvey, A.R.; McNaught, A.I. Spectral Imaging of the Retina. *EYE* **2011**, *25*, 309–320. [CrossRef]
6. Wang, X.-D.; Wolfbeis, O.S. Optical Methods for Sensing and Imaging Oxygen: Materials, Spectroscopies and Applications. *Chem. Soc. Rev.* **2014**, *43*, 3666–3761. [CrossRef] [PubMed]
7. Lehner, P.; Staudinger, C.; Borisov, S.M.; Klimant, I. Ultra-Sensitive Optical Oxygen Sensors for Characterization of Nearly Anoxic Systems. *Nat. Commun.* **2014**, *5*, 4460. [CrossRef]
8. Boles, M.A.; Ling, D.; Hyeon, T.; Talapin, D.V. The Surface Science of Nanocrystals. *Nat. Mater.* **2016**, *15*, 141–153. [CrossRef]
9. Qian, L.; Zheng, Y.; Xue, J.; Holloway, P.H. Stable and Efficient Quantum-Dot Light-Emitting Diodes Based on Solution-Processed Multilayer Structures. *Nat. Photonics* **2011**, *5*, 543–548. [CrossRef]
10. Nozik, A.J. Quantum Dot Solar Cells. *Phys. E Low Dimens. Syst. Nanostruct.* **2002**, *14*, 115–120. [CrossRef]
11. Kang, T.; Um, K.; Park, J.; Chang, H.; Lee, D.C.; Kim, C.-K.; Lee, K. Minimizing the Fluorescence Quenching Caused by Uncontrolled Aggregation of CdSe/CdS Core/Shell Quantum Dots for Biosensor Applications. *Sens. Actuators B Chem.* **2016**, *222*, 871–878. [CrossRef]
12. Wu, P.; Yan, X.-P. Doped Quantum Dots for Chemo/Biosensing and Bioimaging. *Chem. Soc. Rev.* **2013**, *42*, 5489–5521. [CrossRef] [PubMed]
13. Peng, X.; Manna, L.; Yang, W.; Wickham, J.; Scher, E.; Kadavanich, A.; Alivisatos, A.P. Shape Control of CdSe Nanocrystals. *Nature* **2000**, *404*, 59–61. [CrossRef]
14. Bawendi, M.G.; Carroll, P.J.; Wilson, W.L.; Brus, L.E. Luminescence Properties of CdSe Quantum Crystallites: Resonance between Interior and Surface Localized States. *J. Chem. Phys.* **1992**, *96*, 946–954. [CrossRef]
15. Murphy, C.J. Peer Reviewed: Optical Sensing with Quantum Dots. *Anal. Chem.* **2002**, *74*, 520A–526A. [CrossRef]
16. Murray, C.B.; Norris, D.J.; Bawendi, M.G. Synthesis and Characterization of Nearly Monodisperse CdE (E = Sulfur, Selenium, Tellurium) Semiconductor Nanocrystallites. *J. Am. Chem. Soc.* **1993**, *115*, 8706–8715. [CrossRef]
17. Wang, X.; Qu, L.; Zhang, J.; Peng, X.; Xiao, M. Surface-Related Emission in Highly Luminescent CdSe Quantum Dots. *Nano Lett.* **2003**, *3*, 1103–1106. [CrossRef]
18. Sowers, K.L.; Hou, Z.; Peterson, J.J.; Swartz, B.; Pal, S.; Prezhdo, O.; Krauss, T.D. Photophysical Properties of CdSe/CdS Core/Shell Quantum Dots with Tunable Surface Composition. *Chem. Phys.* **2016**, *471*, 24–31. [CrossRef]
19. Seo, J.; Raut, S.; Abdel-Fattah, M.; Rice, Q.; Tabibi, B.; Rich, R.; Fudala, R.; Gryczynski, I.; Gryczynski, Z.; Kim, W.-J.; et al. Time-Resolved and Temperature-Dependent Photoluminescence of Ternary and Quaternary Nanocrystals of $CuInS_2$ with ZnS Capping and Cation Exchange. *J. Appl. Phys.* **2013**, *114*, 094310. [CrossRef]
20. Rice, Q.; Raut, S.; Chib, R.; Gryczynski, Z.; Gryczynski, I.; Zhang, W.; Zhong, X.; Abdel-Fattah, M.; Tabibi, B.; Seo, J. Fractional Contributions of Defect-Originated Photoluminescence from $CuInS_2$/ZnS Coreshells for Hybrid White LEDs. *J. Nanomater.* **2014**, *2014*, 1–7. [CrossRef]
21. Sillen, A.; Engelborghs, Y. The Correct Use of "Average" Fluorescence Parameters. *Photochem. Photobiol.* **1998**, *67*, 475–486.
22. Lakowicz, J.R. *Principles of Fluorescence Spectroscopy*, 3rd ed.; Springer: New York, NY, USA, 2010.
23. Yu, W.W.; Qu, L.; Guo, W.; Peng, X. Experimental determination of the extinction coefficient of CdTe, CdSe and CdS nanocrystals. *Chem. Mater.* **2003**, *15*, 2854–2860. [CrossRef]
24. Yu, W.W.; Qu, L.; Guo, W.; Peng, X. Experimental Determination of the Extinction Coefficient of CdTe, CdSe and CdS Nanocrystals. *Chem. Mater.* **2004**, *16*, 560. [CrossRef]
25. O'Donnell, K.P.; Chen, X. Temperature Dependence of Semiconductor Band Gaps. *Appl. Phys. Lett.* **1991**, *58*, 2924–2926. [CrossRef]
26. Shibata, H. Negative Thermal Quenching Curves in Photoluminescence of Solids. *Jpn. J. Appl. Phys.* **1998**, *37*, 550–553. [CrossRef]
27. Jones, M.; Nedeljkovic, J.; Ellingson, R.J.; Nozik, A.J.; Rumbles, G. Photoenhancement of Luminescence in Colloidal CdSe Quantum Dot Solutions. *J. Phys. Chem. B* **2003**, *107*, 11346–11352. [CrossRef]
28. Nirmal, M.; Norris, D.; Kuno, M.; Bawendi, M.; Efros, A.L.; Rosen, M. Observation of the "Dark Exciton" in CdSe Quantum Dots. *Phys. Rev. Lett.* **1995**, *75*, 3728–3731. [CrossRef] [PubMed]